communications materials

A Nature Portfolio journal

Article

https://doi.org/10.1038/s43246-025-00850-y

Properties governing dry-state stability of RNA in amorphous sugar formulations

Tyler J. Gonzalez & Thomas C. Boothby

Formulation with non-crystalline amorphous solids, is a common strategy employed in nature for organisms to protect themselves from desiccation. These organisms typically accumulate high levels of disaccharides, such as trehalose, to achieve these amorphous states. These strategies have previously been co-opted for the stabilization of protein-based therapeutics, however, the applicability of amorphous sugars in the stabilization of RNA has not been fully explored. Here, we show that disaccharides improve stability of dry RNA up to a threshold, past which degradation occurs. This degradation is correlated with the water mass of dry samples as well as the dynamics of solid-state crystallization. Reducing water content and accelerating the transition from an amorphous to crystalline state increases RNA protection. Our results demonstrate that amorphous sugars are a cost-effective and efficient means of stabilizing RNA in a dry state outside of the cold-chain. Furthermore, we identify material properties of these dry materials that modulate the stability of embedded RNA.

In recent years, RNA-based therapeutics have demonstrated their importance in modern medicine, offering several benefits over traditional vaccines and therapies[1]. However, a major drawback of RNA-based therapeutics is the inherent instability of RNA, requiring sub-zero storage temperatures and a reliable cold-chain[2]. Improving storage methodologies of RNA to allow for long-term refrigerated, room temperature storage, or even preservation under elevated temperatures would address one of the largest drawbacks to mRNA-based therapeutics and increase ease of distribution in developed, developing, and remote parts of the world.

RNA can undergo several different reactions in the hydrated state, rendering it non-functional[3]. These reactions include oxidation, causing a variety of modifications to nucleotide bases which can disrupt translation[4], and hydrolysis, in which the hydroxyl group on the 2′ carbon of ribose undergoes a hydrolysis reaction with backbone phosphate, resulting in cleavage of the RNA strand[5,6]. Of these two processes, self-hydrolysis is more common in the absence of free radicals, due to the hydrolysis reaction being catalyzed by water[5,7]. Importantly, intrinsic RNA features such as length[3] and secondary structure[6] can influence the rate of degradation of a given RNA strand. Given RNA's reactivity with water, one potential solution to long-term RNA preservation is storage in the dry state[7–10]. Dry state storage has been used to preserve sensitive biomolecules, such as proteins, for extended periods outside of the cold-chain[11–13]. Typically, preserving sensitive proteins in the dry state has been achieved by using protectants that stabilize biomolecules and prevent unfolding/aggregation in the dry state[11,14–16]. However, the direct loss of water does not damage nucleotides, but provides stabilization even without the use of protectants[17,18]. For example, Marrone and Ballantyne observed that hydrated DNA was completely degraded after 33 h at 65 °C, while dry DNA was still intact after 700 h at 65 °C[18].

In addition to any basal stability of dry RNA, further improving stability would be a boon for long-term storage and transport. Such technologies exist, such as Biomatrica's RNAstable® and Imagene's RNAshell®, but are proprietary chemical formulations and/or require access to advanced equipment[7–10]. In nature, some organisms that survive extreme drying, or desiccation, are capable of preserving RNA for years or even decades in the dry state, requiring this RNA for recovery after rehydration[19–25]. From these studies, it is clear that intact RNA is needed for some desiccation-tolerant organisms to recover from the dry state. By adopting strategies employed by these organisms, it may be possible to improve the stability of dry RNA products using non-toxic, readily available compounds.

A seemingly universal strategy for mitigating the deleterious effects of desiccation is the accumulation of protectant cosolutes, which stabilize and prevent damage to sensitive biomolecules during drying[26–29]. These protectants are diverse[28,30], but two of the most common and well-studied protectants are the non-reducing disaccharides trehalose[31–36] and sucrose[27,37,38]. These sugars are vital for desiccation survival in many organisms[27,31–37], and are also capable of stabilizing desiccation-sensitive proteins and membranes during drying[27,32,37–40]. Due to these properties, these sugars are commonly used to stabilize biomolecules during drying and freezing[14,41,42].

Whereas the importance of disaccharides such as trehalose and sucrose in desiccation tolerance is well accepted[26,27,29,32], the efficacy of these two protectants in stabilizing RNA is not well understood. Studies have reported

Department of Molecular Biology, University of Wyoming, 1000 E. University Ave, Laramie, WY, USA.
e-mail: tboothby@uwyo.edu

that trehalose has a positive effect on RNA stability in the dry state, but these studies only test one concentration of trehalose, without replication or statistical analysis[43] or only quantify RNA recovery following extraction from paper matrices[44]. Given previous work establishing the importance of disaccharides and RNA for desiccation survival in organismal systems, as well as the established use of disaccharides as desiccation protectants, disaccharides may be promising candidates for RNA stabilization in the dry state.

We find that both total RNA and coding RNA degrade significantly less when dry relative to when hydrated, and are further stabilized by trehalose and sucrose in a concentration-dependent fashion, up to a point. We find that the degradation of RNA at higher sugar concentrations is linked to not only the water mass in samples, but also to the dynamics and properties of solid-state crystallization. Our study demonstrates that sugar-based protection of RNA is a viable means for increasing short- as well as long-term stability in the dry state, and that considering sugar concentration, water content, and crystallization dynamics of the resulting formulations is essential for maximizing RNA stability.

Results

The dry state provides protection to RNA

To assess the effects of air-drying on the integrity of RNA, we used two different assays, RNA integrity number equivalent[45] (RINe, Fig. 1a) quantification and an in vitro translation assay (Fig. 1b), which we validated using hydrated total or coding RNA, respectively. For both RINe and the in vitro translation assay, samples are normalized to fully intact RNA, proving the highest observed RINe or fluorescence after translation. In general, RINe is typically utilized as quality control for RNA extraction prior to downstream RNA analyses, such as RT-qPCR and transcriptomics. RINe analysis results in a number between 1 and 10, where 10 is fully intact RNA and 1 is completely degraded RNA, based on the sizes of ribosomal subunits present on the gel[45] (Fig. 1a). In general, a RINe >7 is suitable for downstream applications, while RNA of a lower RINe is typically too degraded[45]. In contrast, the in vitro fluorescence assay is a direct measure of the amount of protein product being produced from RNA present, and is a more direct measure of mRNA function in contrast to RINe. All raw RINe and fluorescence measurements can be found in File S1. As expected, both hydrated total and coding RNA degrade as time and temperature increase (Fig. 1c, d). Conditions known to accelerate RNA degradation (such as modulating pH and Mg^{2+} concentration[3,5]) likewise result in increased degradation in our assays (Supplementary Fig. 1).

After determining that the two assays mentioned above can reliably measure the integrity and translatability of total and coding RNA, we next determined the effects of vacuum desiccation on total and coding RNA (See Methods, Fig. 2a). Neither total nor coding RNA show significant degradation when compared to control RNA (freshly thawed from −80 °C, Fig. 2b, d −23 °C Day 0). This demonstrates that the process of drying via vacuum centrifugation does not perturb RNA integrity or translatability in the short term, aligning with previous work regarding RNA stability during vacuum drying[7,9].

Given the stability of RNA during drying, we wondered if the removal of water is sufficient to keep RNA stable long-term in the dry state. We performed time courses similar to experiments on hydrated RNA (Fig. 1c, d) to determine if RNA in the dry state exhibited increased stability. Both dry total RNA (Fig. 2b) and dry coding RNA (Fig. 2d) exhibit no significant degradation at 23 °C even after 7 days. To simulate aging, we also tested dry RNA stored at 37 and 60 °C. At 37 °C, both total and coding RNA show significant decreases in integrity or translatability during the time course (Fig. 2b, d −37 °C). As expected, the 60 °C time course exhibited the largest degree of degradation, with both types of RNA exhibiting the highest degradation at each time point tested relative to other temperatures (Fig. 2b, d −60 °C).

When compared to hydrated RNA under the same conditions (Fig. 1b, d), dry RNA exhibits a significant increase in stability at several time points and temperatures (Fig. 2c, e). These results reinforce that drying via vacuum centrifugation is not in and of itself damaging to RNA and that the dry state has a long-term stabilizing effect on both total RNA integrity and coding RNA translatability relative to hydrated conditions.

Trehalose and sucrose enhance inherent RNA stability in the dry state

Given that in vitro, RNA still degrades over time in the dry state (Fig. 2b, d), we hypothesize that the protectants trehalose and sucrose may further improve the stability of dry RNA. In order to achieve sufficient degradation in shorter time periods, 60 °C for 24 h were selected as a time and temperature point, which results in moderate degradation of dry RNA (Fig. 2b, d). No effect on RNA stability is observed for either sugar in the hydrated state (Supplementary Fig. 2a–d), implying that these sugars are not protective to hydrated RNA, and that both sugars are free of any RNase contamination as only RNA translation is affected by high sugar concentration (Supplementary Fig. 3a–d).

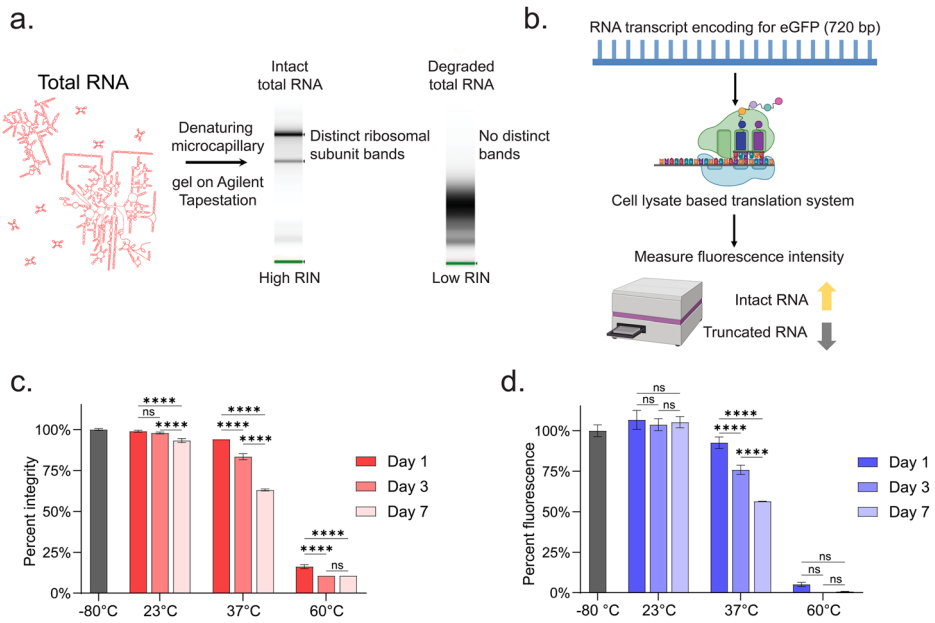

Fig. 1 | Degradation of hydrated total RNA and coding RNA. RNA was analyzed using RNA integrity number (**a**) and in vitro translation (**b**) assays. Degradation over a 7-day time course at 23, 37, and 60 °C for hydrated total (**c**) and coding (**d**). ****$P < 0.0001$, ***$P < 0.001$, **$P < 0.01$, *$P < 0.05$ analyzed using Tukey's multiple comparisons test following two-way ANOVA. All error bars are standard deviation. Total RNA is represented as red, coding RNA as blue. Created in BioRender.

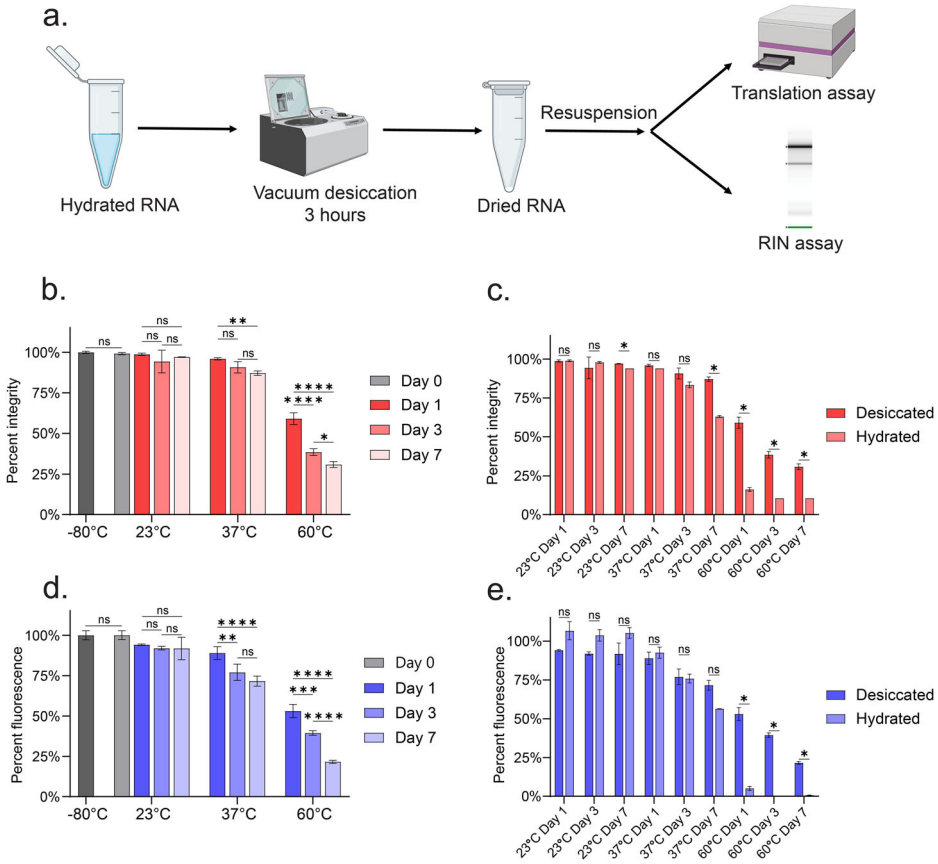

Fig. 2 | RNA degradation over time in the dry state. Drying regime used to dry RNA (**a**) and 7-day time course of dry total (**b**, $P < 0.0001$ for both interaction and main effects) and coding (**d**, $P < 0.0001$ for both interaction and main effects) RNA at 23, 37, and 60 °C. Comparison between hydrated 7-day time courses (Fig. 1c, d) and desiccated 7-day time course (**c**, **e**) for total and coding RNA. $^{****}P < 0.0001$, $^{***}P < 0.001$, $^{**}P < 0.01$, $^{*}P < 0.05$ analyzed using Tukey's multiple comparisons test following two-way ANOVA or Welch's unpaired *t*-test with correction for multiple comparisons (**c**, **e**). All error bars are standard deviation. Total RNA is represented as red, coding RNA as blue. Created in BioRender.

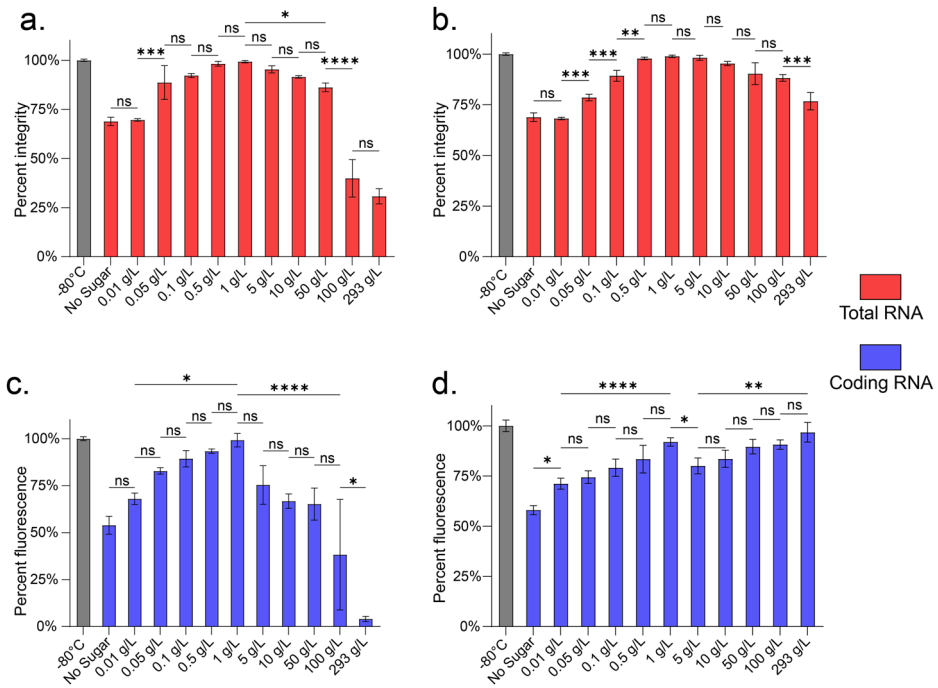

Fig. 3 | Dry RNA degradation with varying concentrations of disaccharides. Protection of dry total RNA (red) with sucrose (**a**) and trehalose (**b**). Protection of coding RNA (blue) with sucrose (**c**) and trehalose (**d**). $^{****}P < 0.0001$, $^{***}P < 0.001$, $^{**}P < 0.01$, $^{*}P < 0.05$ analyzed using Tukey's multiple comparisons test following one-way ANOVA. ANOVA $P < 0.0001$ for all trials. All error bars are standard deviation. Total RNA is represented as red, coding RNA as blue.

We observe that both sugars provide significant protection to both dry total and coding RNA, with protection increasing with sugar concentration up to 1 g/L (Fig. 3—No Sugar to 1 g/L). Past 1 g/L, RNA degradation begins to increase for most trials, demonstrating a non-monotonic trend in protection (Fig. 3—1 to 293 g/L). The degradation past 1 g/L is more pronounced in the sucrose trials, with much larger drops in protection than in trehalose trials (Fig. 3a, c) and degradation reaching near hydrated levels (Fig. 1b, d). Coding RNA and trehalose is an exception to this trend, exhibiting an immediate loss in protection past 1 g/L, but then building up to high levels of protection with higher trehalose concentration (Fig. 3d). It should be noted that mixtures containing protectant disaccharides have previously been shown to also display non-monotonic trends for protein

stabilization[13,46,47]. Extending our measurements to quantify the degradation rate of RNA in different formulations, we find similar results with dry samples stored at 37 °C for 3 weeks, albeit with less degradation at higher sugar concentrations (Supplementary Fig. 4). In addition, we observe similar sugar protection with a smaller (330 bp) RNA (Supplementary Fig. 5a, b), suggesting that RNA size may not play a role in governing RNA-sugar stability.

Combined, these data demonstrate that trehalose and sucrose confer protection to total and coding RNA in a dry state, but at higher concentrations, these protective effects can be counteracted by an emergent perturbing effect that is different between the two sugars. These results also indicate that while offering similar protection at optimal concentrations, trehalose outperforms sucrose at high concentrations as a desiccation protectant for both total and coding RNA under the conditions used here (Supplementary Fig. 2e, f).

Retained water correlates with RNA degradation for most samples

After determining that trehalose and sucrose are capable of protecting both total RNA and coding RNA, we sought to investigate possible mechanisms underlying why low levels of disaccharides are protective to dry RNA, but become detrimental at higher concentrations. We performed differential scanning calorimetry experiments to analyze the glassy properties of dry sucrose at higher concentrations (Supplementary Fig. 6), which have been linked to dry state stability[47,48]. We find that while the glass transition temperature did vary with sugar concentration (Supplementary Fig. 6a), it exhibited a non-significant correlation with RNA degradation (Supplementary Fig. 6c), while glass former fragility exhibited no change with concentration or relationship to RNA degradation (Supplementary Fig. 6b, d). Given both disaccharides' ability to retain water during drying[47] as well as water's role in facilitating RNA degradation[5] we next wished to determine if water is related to the observed pattern of protection and degradation.

To explore the role of water in the degradation of RNA in the dry state, we quantified the stability of dry total RNA with varying drying times after 24 h at 60 °C (Fig. 4a). Unsurprisingly, we find that reducing drying times, and thus increasing residual water, results in increasing degradation for total RNA, indicating that residual water in the dry state can promote RNA degradation. We find similar results for dry RNA held at 60 °C at varying relative humidities, with higher humidities resulting in increasing RNA degradation in the dry state (Supplementary Fig. 7a, b). Unsurprisingly, we also observe an increase in coordinated water in the hydrated state as sugar concentration increases (Supplementary Fig. 8c–f), correlating strongly with degradation in the dry state (Supplementary Fig. 9).

After validating that residual water can cause degradation, we next analyzed the water content present in dry sugar samples using Karl–Fischer Coulometry (Supplementary Fig. 7c–f). Sample sizes were scaled up by a factor of 10, RNA excluded, and drying time increased to 24 h (see Methods) to allow for a wider concentration of sugars to be tested (Supplementary Fig. 10). We found no differences in the percent water between sugars with RNA dried in 7 uL for 3 h and sugar alone dried in 70 uL for 24 h (Supplementary Fig. 11), indicating that these two drying regimes are equivalent in terms of percent water retained.

Unsurprisingly, we find that water mass exhibits a negative correlation with degradation for all trials (Fig. 4b–d and Supplementary Fig. 12) except for coding RNA and trehalose (Fig. 4e), suggesting a relationship between water mass and RNA degradation. This relationship is also present for 7 uL samples (Supplementary Fig. 13). However, since percent water is similar between samples (Supplementary Figs. 7, 10, 11), we hypothesize that if increased water mass is a driver of RNA instability, there must be some mechanism that promotes differential interactions between RNA and excess water (Supplementary Fig. 14) in the dry state and causes the differences in RNA degradation observed between dry trehalose and sucrose at high sugar concentrations (Fig. 3—293 g/L).

Disaccharide crystallization dynamics mirror differences in RNA integrity at high sugar concentrations

To understand how the same mass of water in a sucrose versus trehalose sample might be differentially accessing RNA, we wanted to further investigate the physical nature of our resulting sugar matrices. One possible mechanism that could promote water–RNA interactions is the crystallization of the disaccharides, since crystalline trehalose and sucrose are known to exhibit differences in the distribution of water across their matrices[49–51] and form different amorphous/crystalline domains at similar water content[51].

In order to determine if our samples were undergoing crystallization, we performed X-ray diffractometry on 293 g/L dry samples after 24 h at 60 °C. We find that both sugars exhibit sharp, defined peaks, indications of crystallinity (Fig. 5a, b). Importantly, peak positions suggest that trehalose exists in the dihydrate form[52,53] while sucrose exists in the anhydrous form[54].

After observing that our samples were indeed crystalline, we wished to gain insights into how quickly crystallization was occurring at 60 °C, and the rate at which crystals formed. To achieve this, we utilized DSC to monitor heat flow during an isothermal hold at 60 °C. Both sugars exhibit a spontaneous exothermic peak, albeit at different times and of different sizes, indicating that our samples are initially amorphous (non-crystalline), and as they age in the dry state, undergo solid-state crystallization at different rates(Fig. 5c)[55]. Trehalose crystallizes rapidly (Fig. 5c and Supplementary Table 1), while sucrose crystallizes more slowly (Fig. 5c and Supplementary Table 2).

Importantly, faster crystallization dynamics (as observed with trehalose) are known to result in more homogenous dispersal of impurities relative to slow dynamics (as observed with sucrose)[56]. These results suggest that while the total mass of water in trehalose and sucrose samples are indistinguishable, differences in water distribution, as a result of different crystallization dynamics, drive differences in RNA protection.

Discussion

While the chemistry and molecular behavior of RNA is well studied in the hydrated state, less is known about RNA behavior in the dry state. Fortunately, a significant amount of research into solid-state reaction kinetics has been performed on DNA, providing general insights into nucleic acids in the dry state[18,57]. Relevant to RNA is the notion that hydrolysis reactions can still occur in the dry state[18], utilizing residual water remaining after drying, and have been shown to occur in dry DNA, albeit at lower rates than hydrated samples[18]. This aligns well with the differences in degradation seen between hydrated and dry RNA in our study, where the removal of the majority of water decreases degradation but does not halt it altogether. However, one surprising result is the similarities between the degradation of total (Figs. 1c, 2b) and coding (Figs. 1d, 2d) RNA. Given what is known about the effect of length[3] and secondary structure[6] on RNA degradation, we were surprised to see such similar degradation between a longer, highly structured RNA (rRNA quantified in the RIN assay, Fig. 1a) and a shorter, most-likely less structured RNA (RNA encoding for eGFP, Fig. 1b). Since RNA length increases the chance of self-hydrolysis along the RNA strand[3], while secondary structure makes an RNA less prone to this reaction[6], it may be possible that these two factors "cancel-out", resulting in similar degradation for total and coding RNA. Of course, it is also likely that the two assays exhibit differences in the sensitivity of RNA degradation, and they cannot truly be compared directly to one another.

While we do observe significant protection by just drying RNA (Fig. 2c, e), additional time or increased temperature can still result in RNA degradation (Fig. 2b, d). The simple addition of trehalose or sucrose can significantly improve dry state stability (Fig. 3), allowing for dry RNA to not only be stable at room temperature, but at elevated temperatures. This increased stability in elevated temperatures would be beneficial for the storage and transport of RNA, especially in underdeveloped regions. However, we do observe significant decreases in RNA protection past 1 g/L of sugar. The decrease in protection past 1 g/L correlates with water mass for most samples (Fig. 4), suggesting excess water could play a role in

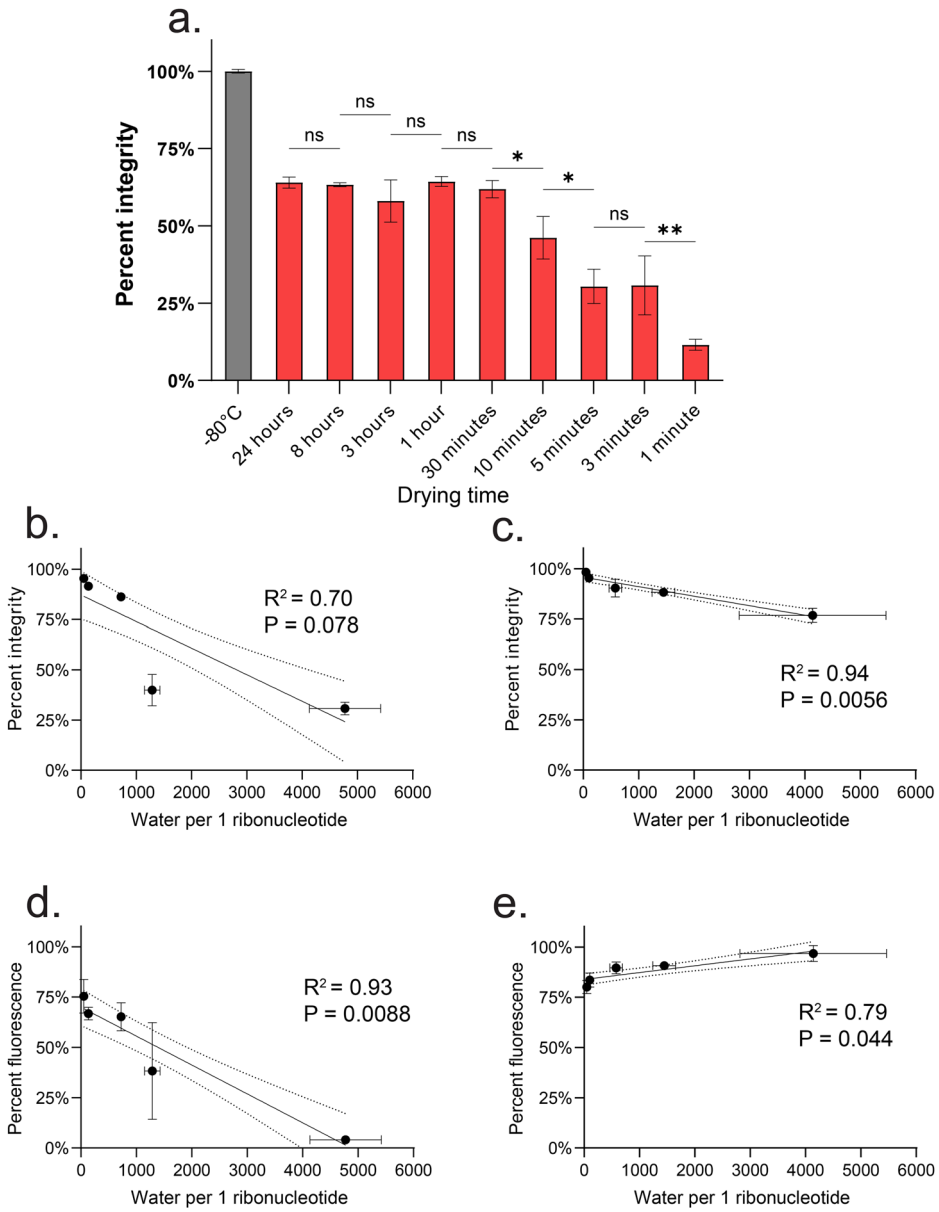

Fig. 4 | Effect of drying time on dry total RNA degradation and retained water of sugar mixtures. Twenty-four-hour 60 °C trials of dry total RNA degradation at varying drying times (**a**). Retained water of 70 uL buffer with varying concentrations of sucrose (**b**) or trehalose (**c**) compared to total RNA degradation. Retained water of 70 uL buffer with varying concentrations of sucrose (**d**) or trehalose (**e**) compared to coding RNA degradation. All sugar concentrations from left to right are 5, 10, 50, 100, and 293 g/L. ****$P < 0.0001$, ***$P < 0.001$, **$P < 0.01$, *$P < 0.05$ analyzed using Tukey's multiple comparisons test following one-way ANOVA (**a**). R^2 and P values are Pearson correlations, and lines of best fit are simple linear regressions with 95% confidence intervals (**b**–**e**). One-way ANOVA $P < 0.0001$. Correlations for 7 uL samples can be found in S11. All error bars are standard deviation.

degradation. However, this excess water should be evenly dispersed across the sugar matrix, indicating that another mechanism must allow for excess water to interact with RNA. Performing DSC analysis on dry sucrose samples shows only a weak correlation between protection and glass transition temperature (Supplementary Fig. 6c) with glass transition temperature, although glass transition temperature does vary with sugar concentration (Supplementary Fig. 6a) despite maintaining similar water content. In contrast, we observe no relationship between sugar concentration and glass former fragility (Supplementary Fig. 6b) or between protection and glass former fragility (Supplementary Fig. 6d). Importantly, all sucrose glass transitions were below 0 °C (Supplementary Fig. 6a), and all experiments occurred well above this temperature. It is known that temperatures above a material's glass transition can favor an amorphous-to-crystal solid-state transition[58], which provides a mechanism that may allow water to interact with entrapped RNA.

Crystallization is well understood to be capable of excluding impurities from a growing crystalline matrix[59,60], providing a hypothetical mechanism by which RNA and increased residual water are brought into proximity, thereby accelerating degradation. Importantly, it is known that the rate of crystallization can affect the expulsion of impurities from the growing crystal, with faster crystallization leading to more impurities being trapped within crystals[56]. The "quick" crystallization of trehalose when compared to sucrose may result in more RNA and water entrapped within the matrix, while the "slow" crystallization of sucrose may result in the greater exclusion of RNA and water (Fig. 5d). This would result in greater water–RNA interactions, explaining the near hydrated levels of degradation observed with high levels of sucrose (Fig. 3a, c).

Additionally, trehalose and sucrose are known to incorporate different amounts of water into their crystalline matrices. XRD data (Fig. 5a, b) indicate that trehalose crystallized into its common dihydrate form[53], while sucrose crystallized into its common anhydrous form[61]. It is known that crystalline trehalose can adsorb water in order to satisfy the amount of water required to form the dihydrate[62–64]. Given this, it's also possible that the formation of trehalose dihydrate is sequestering water away from entrapped RNA, while the slower formation of anhydrous sucrose is expelling water and RNA forcing the two to interact (Fig. 5d). Additionally, trehalose and sucrose crystal growth can be slowed at reduced temperatures[61,64], possibly explaining the lack of degradation seen at higher sugar concentrations during 3 week degradation experiments at 37 °C (Supplementary Fig. 4), but similar protection.

While we have some evidence for the possible mechanisms by which high sugar concentrations result in RNA degradation, the mechanism by

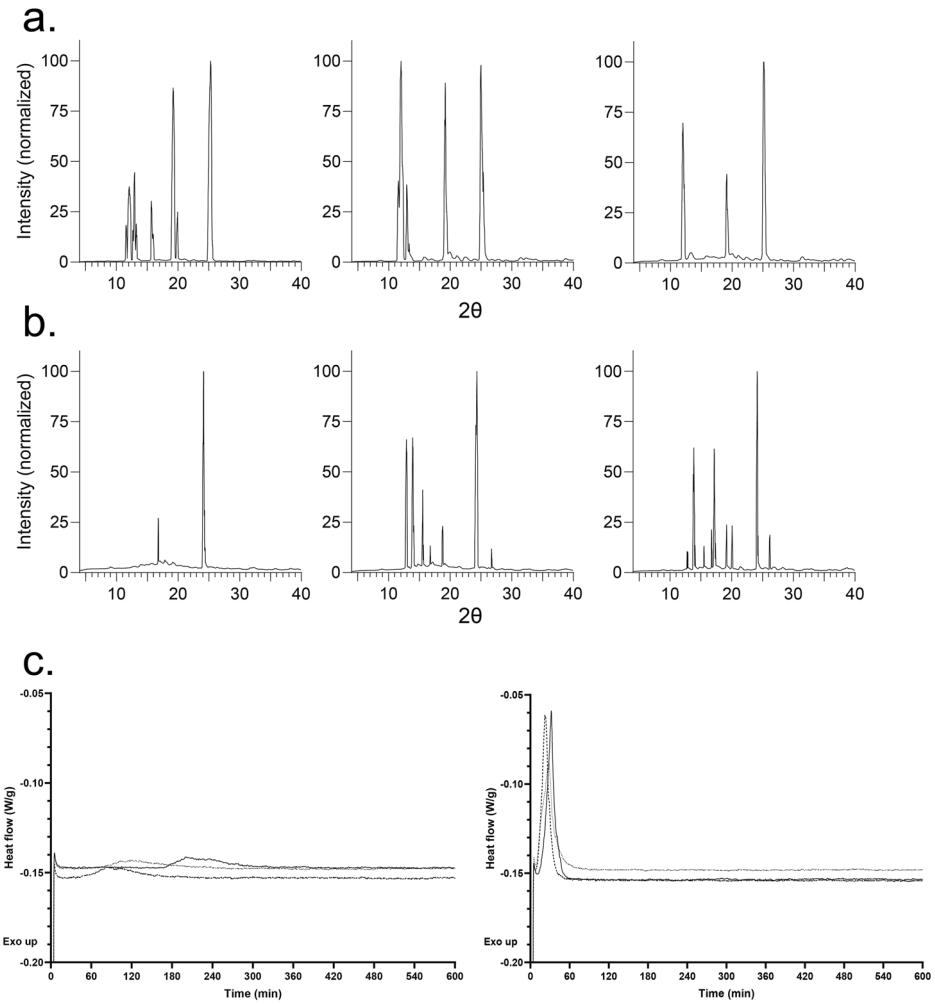

Fig. 5 | Crystallization dynamics of sugar mixtures. XRD of aged (24 h, 60 °C) sucrose (**a**) and trehalose (**b**) in triplicate. Sucrose peaks (**a**) align with reported XRD spectra of anhydrous sucrose[54], and trehalose (**b**) exhibit peaks (near 16 and 24 2θ) indicative of the dihydrate form[52,53]. Heat flow of 293 g/L of dry sucrose (left) and trehalose (right) during 24 h isothermal holds at 60 °C (**c**). Thermograms have been expanded for better detail of crystallization peaks. Each line represents one replicate. Full thermograms can be found and analyses can be found in Supplementary Fig. 15 and Supplementary Tables 1, 2.

which RNA is stabilized by these disaccharides is less clear. Importantly, we find optimal sugar protection at 1 mg/mL for both total (Fig. 3a, b) and coding (Fig. 3c, d) RNA, as well as smaller 330 bp RNA (Supplementary Fig. 5a, b). In addition, optimal sugar protection shifts depending on RNA concentration (Supplementary Fig. 5c, d), suggesting that a certain amount of sugar per nucleotide is important for protection, irrespective of RNA size. It may be possible that disaccharides are replacing the water around RNA during drying, preventing possible hydrolysis reactions (Fig. 6). Indeed, the optimal sugar concentration for our mixtures yields a nucleotide:sugar ratio of 1:7.3, similar to the amount of water molecules that hydrate an individual nucleotide (4–7 water molecules depending on nucleotide and base pairing)[65,66]. Not only is water replacement an already established hypothesis for the protection of other biomolecules in the desiccation tolerance field[67,68], it is also known that disaccharides can replace hydrating water around nucleotides in solution, destabilizing secondary structure and lowering melting temperatures[69,70]. Overall, our study largely agrees with the significant amount of previous work done on protein stabilization in amorphous glasses, with protection potentially being caused by sugars displacing residual water around RNA, a well established theory for sugar-based dry protein protection[67,68] and degradation being caused by unwanted crystallization with differing dynamics between the two sugars, again aligning with previous hypotheses addressing trehalose's properties that make it a superior protectant[51].

This study reinforces that dry storage of RNA is viable for maintaining RNA integrity outside of the cold-chain, at ambient or even elevated temperatures. Furthermore, while RNA is stabilized by the removal of water, known desiccation protectants, trehalose and sucrose, provide further dry-state stabilization and longevity at elevated temperatures, and a 1:7 nucleotide:sugar ratio offers the most robust protection. We find that crystallization of these disaccharides appears to be detrimental to RNA stability in the dry state, but reducing disaccharide concentration to minimize excess water and avoiding crystallization can greatly reduce this degradation. These findings may provide additional avenues for the delivery and storage of RNA-based therapeutics, which could be particularly beneficial in remote and developing parts of the world as well as in austere conditions. However, it is important to note that RNA stabilization is just one factor in the preservation of RNA therapeutics, and the stabilization of the delivery vehicle is equally important. While both disaccharides have been shown to stabilize dry membranes[39,71], further experiments will be needed to determine the capability of trehalose and sucrose in stabilizing RNA and a delivery vehicle in a linked system before dry-state stabilization of RNA therapeutics can be achieved.

Methods

Total RNA

Human total RNA from K-562 leukemia cell lines was purchased from Invitrogen (AM7832) and used for all total RNA experiments.

Coding RNA production

DH10b *E. coli* transformed with pET28a:GFP (Addgene #60733) were grown for 16 h at 37 °C in Luria-Bertani (LB) broth at 250 RPM in a shaking incubator. After 16 h of growth, plasmid DNA was extracted using commercial plasmid miniprep kits (QIAprep Spin Miniprep Kit – 27104). pET28a:GFP was linearized with an overnight restriction digest utilizing BamHI-HF (NEB) at 37 °C. DNA was then cleaned and concentrated using Zymo Oligo Clean and Concentrator (D4060), and eluted in 9 uL nuclease-

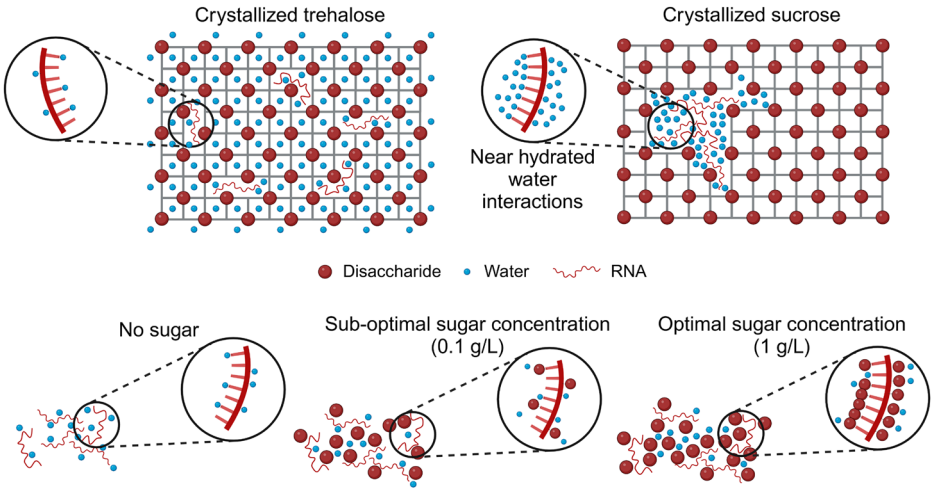

Fig. 6 | Schematic of the proposed mechanism of protection via water replacement and degradation due to water interaction caused by crystallization. Larger red spheres represent disaccharides, smaller blue spheres represent water, and red lines represent RNA. Created in BioRender.

free water. Linear DNA concentration and purity was quantified on a Thermo Scientific NanoDrop One. Linearized plasmid was then transcribed to coding RNA utilizing an Invitrogen MEGAscript T7 transcription kit (AM1334), with a reaction time of 4 h. After transcription, RNA was purified with an Invitrogen MEGAclear transcription clean-up kit (AM1908), and eluted in Invitrogen's The RNA Storage Solution, pH 6.5 (TRss, AM7001) utilizing the second elution method described in the MEGAclear clean-up kit, producing an RNA encoding for eGFP (720 bp). RNA quantification and purity was then determined using a Thermo Scientific NanoDrop One. Samples were diluted to 1000 ng/uL (1 mg/mL) with the addition of TRss. After quantification, RNA was stored at −80 °C until use.

Assessment of total RNA integrity

RNA integrity number equivalent (RINe) was determined using an Agilent 4200 Tapestation, utilizing Agilent high-sensitivity RNA screentape (5067-5579). Total RNA (at 1 mg/mL) was first diluted in nuclease-free water to reach the required functional range of the instrument (1–25 ng/uL) before analysis. About 2 uL of dilute RNA was mixed with 1 uL high-sensitivity screentape buffer and prepared according to the manufacturer's protocol. A high-sensitivity ladder was prepared in an identical manner, with 2 uL of ladder mixed with 1 uL of high-sensitivity buffer before analysis. An initial RINe was taken for each total RNA sample before the experiment began, and then compared to the experimental trials.

Quantification of coding-RNA translatability

In vitro translation was performed utilizing Promega's Rabbit Reticulocyte Lysate system (L4960). Reaction size was scaled down by 50%, for a total reaction volume of 25 uL. About 7 uL of coding RNA at a concentration of 142 ng/uL (1 ug) was combined with 0.5 uL premixed amino acid solution and 17.5 uL rabbit reticulocyte lysate, mixed gently, and incubated at 30 °C for 90 min. After 90 min, 20 uL from each reaction was added to individual wells of a black 384-well microplate (Greiner, 781900), spun at 900 rpm (174 rcf) for 3 min before the fluorescence of each well was measured using a Tecan CytoSpark plate reader. Each experiment included a control translation with no added RNA, which was used for background subtraction. All translation experimental trials were paired to identical frozen controls.

Desiccation of RNA

Here, we opted to use vacuum drying instead of lyophilization or spray-drying, due to the low cost, ease of operation, and more widespread availability of vacuum desiccators compared to the aforementioned techniques. For drying, 1 uL (1 ug/uL) of RNA in "the RNA storage solution", pH 6.5, was diluted to a total volume of 7 uL with nuclease-free water before being placed into a Savant Speedvac SC110 concentrator. Vacuum was achieved using a Thermo Scientific OFP400 vacuum pump. Samples were spun under vacuum with no heating for 3 h to achieve desiccation. For rehydration, samples were either rehydrated in 100 uL nuclease-free water (for total RNA samples) or 7 uL nuclease-free water (for coding RNA samples) and allowed to sit for 1 h, before being utilized in their respective assays. During drying, all samples were dried with a consistent volume in the vacuum concentrator, 33 tubes with 7 uL of solution. For experiments that utilized less than this number, additional tubes with nuclease-free water were added for consistency in drying rates.

Heating of RNA

Hydrated samples were stored to minimize evaporation. For 60 °C experiments, hydrated samples were stored in a BioRad C1000 thermocycler for their respective time points. For the 37 and 23 °C hydrated samples, samples were stored in sealed chambers half-filled with water to maintain humidity (RH >95%) and placed in incubators at 37 or 23 °C. For dry samples, all samples were stored in a desiccation chamber with Drierite (RH <15%), before being placed in incubators at their respective temperatures for the indicated time.

Disaccharide preparation

Ten sugar stock solutions (0.01167, 0.05835, 0.1167, 0.5835, 1.167, 5.835, 11.67, 58.35, 116.7, and 342.3 g/L) were made for both trehalose and sucrose utilizing Amsbio 1 M trehalose solution (AMS.TS1M-100) or Sigma-Aldrich BioUltra sucrose (84097) 1 M stock solutions. About 6 uL of each stock solution was mixed with 1 uL of 1 ug/uL RNA, for a total volume of 7 uL, and sugar concentration of 0.01 g/uL, 0.05 g/L, 0.1 g/L, 0.5 g/L, 1 g/L, 5 g/L, 10 g/L, 50 g/L, 100 g/uL and 293 g/L, respectively. Concentrations were chosen not only to test a variety of conditions, but also to include concentrations exhibiting high levels of protection for other biomolecules[39], whole organisms[35], as well as being physiologically relevant[72]. Samples were then dried as previously described, and placed at 60 °C in a sealed glass desiccation chamber for 24 h. After 24 h, samples were cooled to room temperature, and then total RNA samples were rehydrated in 100 uL nuclease-free water, while coding RNA samples were rehydrated in 7 uL nuclease-free water. Samples were then analyzed in their respective assays.

Control of humidity

For experiments with varying humidity, dry RNA samples in open tubes were placed in an ESPEC environmental test chamber (Model BTL-433). To prevent condensation forming on samples at higher humidities, the chamber was preheated to 60 °C without humidity control (resulting in a chamber humidity of 2–8%), and samples equilibrated for 30 min before humidifying at 60 °C. Samples were removed from the chamber after 24 h, and analyzed as described above.

Karl–Fischer coulometry

Karl–Fischer coulometry was performed using a Metrohm Eco-coulometer without a diaphragm utilizing HYDRANAL Coulomat-AG (34836). Generator current was set to 400 mA and I_{pol} was set to 10 uA. Endpoint was set to 50 mV, and stop drift was 5 ug/min. All experiments were carried out at 25 °C with no extraction time. All experiments were blanked in triplicate utilizing an equal volume of 50% methanol and 50% formamide prior to experimental samples being analyzed.

About 7 uL samples were dried as described previously in preweighed Eppendorf tubes. After drying, the dry mass of a sample was determined before 150 uL of anhydrous 50% methanol and 50% formamide was added to the sample. The sample was vortexed until completely dissolved, briefly centrifuged, then drawn into a 250 uL Hamilton Gastight syringe (1725TLL) with a 4-inch 20-gauge needle. The syringe was then weighed, and the sample was injected into the vessel of the coulometer. The empty syringe was then weighed again, and the injected mass determined. For 70 uL samples, the protocol was identical except samples were dried for 24 h and resuspended in 200 uL of a solution which was 50% methanol and 50% formamide.

X-ray diffractometry

The diffraction data were measured for the samples at room temperature on a Bruker D8 Venture Duo diffractometer equipped with a CMOS IμS Mo and Cu sources, and a PHOTON detector. The data were measured using the Cu Kα radiation. The ca. 0.33 mm samples were mounted on a MiTeGen micromount. The samples were centered, and the diffraction data were measured in the 2q range, 4–70° at room temperature.

Mg^{2+}

About 1.11, 11.1, 111, 1.11 M $MgCl_2$ in nuclease-free water solutions were made by serially diluting a 2 M $MgCl_2$ in H_2O solution. Then, 1 uL of 1 ug/uL RNA was added to 9 uL of the respective $MgCl_2$ solution for final molarities of 1, 10, 100 mM, and 1 M. Samples were then placed at 37 °C as previously described. At each time point, samples were removed, and Mg2+ was removed utilizing a MEGAclear transcription clean-up kit. For total RNA experiments, samples were then analyzed, while for coding RNA, samples were concentrated as described previously using an Oligo Clean and Concentrate kit, and then analyzed by translation.

pH

To determine the amount of acid or base to reach a given pH, varying amounts of 1 mM HCl or 1 mM NaOH was added to Invitrogen's 'The RNA Storage Solution', pH 6.5 (AM7001). This was determined on the milliliter scale to achieve an accurate pH measurement, before being reduced by a factor of 1000 for use on the microliter scale. pH setup was identical for both coding and total RNA. pH 4–2:7 TRss:1 mM HCl, pH 5—3:5.5 TRss:1 mM HCl, pH 6—6:4 TRss:1 mM HCl, pH 7—6:2 TRss:1 mM NaOH, pH 8—8.2:3.2 TRss:1 mM NaOH, pH 9—7:3.2 TRss:1 mM NaOH, 4:6 TRss:1 mM NaOH. At all pHs other than 10, NaCl was added to account for the additional Na+ added by NaOH at pH 10. Samples were then placed at 37 °C for 1 day, 3 days, and 7 days.

After each respective time point, samples were removed from the heat and quenched by being brought to 100 uL with Tris-HCl. Then, samples were cleaned utilizing the Zymo Oligo Clean and Concentrate kit. For total RNA, samples were eluted in 10 uL NFW, and then brought to 100 uL with the addition of 90 uL NFW, before analysis. For coding RNA, samples were concentrated after quenching using the Clean and Concentrate kit as described in the concentration protocol.

Small RNA integrity

pET:28a:miniGFP2 construct was produced by Twist Biosciences (File S1) DH5a *E. coli* transformed with pET28a:miniGFP2 were grown for 16 h at 37 °C in Luria-Bertani (LB) broth at 250 RPM in a shaking incubator. After 16 h of growth, plasmid DNA was extracted using commercial plasmid miniprep kits (QIAprep Spin Miniprep Kit—27104). pET28a:GFP was linearized with an overnight restriction digest utilizing XhoI (NEB) at 37 °C. DNA was then cleaned and concentrated using Zymo Oligo Clean and Concentrator (D4060), and eluted in 9 uL nuclease-free water. Linear DNA concentration and purity was quantified on a Thermo Scientific NanoDrop One. The linearized plasmid was then transcribed to coding RNA utilizing an Invitrogen MEGAscript T7 transcription kit (AM1334), with a reaction time of 16 hours. After transcription, RNA was purified with an Invitrogen MEGAclear transcription clean-up kit (AM1908), and eluted in Invitrogen's The RNA Storage Solution, pH 6.5 (TRss, AM7001) utilizing the second elution method described in the MEGAclear clean-up kit, producing a coding RNA of 330 bp in length. RNA quantification and purity was then determined using a Thermo Scientific NanoDrop One. Samples were diluted to 1000 ng/uL (1 mg/mL) with the addition of TRss. After quantification, RNA was stored at −80 °C until use.

Drying and degradation was achieved in an identical manner to previous RNA. This RNA was unable to be used for an in vitro translation assay, so RNA integrity was instead determined via the electropherogram produced by an Agilent Tapestation. RNA (at 1 mg/mL) was first diluted in nuclease-free water to reach the required functional range of the instrument (1–25 ng/uL) before analysis. 2 uL of dilute RNA was mixed with 1 uL high-sensitivity screentape buffer and prepared according to the manufacturer's protocol. A high-sensitivity ladder was prepared in an identical manner, with 2 uL of ladder mixed with 1 uL of high-sensitivity buffer before analysis. All samples were normalized to the lower marker, before being exported as raw electropherograms.

RNA stability was determined by taking the area under the peak at ~330 bp, and comparing it to the area under the curve at sizes below ~330 bp, up until the lower marker. This ratio was then used as an estimate of RNA integrity, with a higher number being more intact (more RNA at 330 bp) and a lower number being less intact (more fragmented RNA of smaller sizes). This was normalized to fully intact frozen RNA.

Differential scanning calorimetry (DSC)

All DSC experiments were performed on a DSC 2500 (TA instruments) with an autoloader. For heat of melting experiments, RNA:sugar mixtures were scaled up by a factor of four for a total volume of 28 uL. Hydrated samples were pipetted into preweighed aluminum Tzero pans, the samples' mass determined, and then hermetically sealed. Samples were cooled at 1 °C per minute to −40 °C, held for 20 min to ensure thermal equilibrium, and then heated at 1 °C per minute to 20 °C. The curve at 0 °C was then integrated to determine the enthalpy of melting in J/g.

For isothermal crystallization experiments, 7 uL of the highest concentration RNA-sugar mixture (293 g/L of sugar) were dried using vacuum centrifugation in preweighed aluminum Tzero pans. Sample mass was determined, and then hermetically sealed samples were heated to 60 °C at a 10 °C per min until 60 °C, and held isothermally for 24 h. Due to the length of time of each run, samples were dried separately. Total liquid volume was kept consistent, as described under the desiccation protocol. For determining onset/endset times and enthalpy of crystallization, onset/endset analysis were performed utilizing Trios software. Transition starts/ends were adjusted to best follow the curve, and the onset/endset taken. Those bounds were then used to determine the start and end of enthalpy integration.

For dry state analyses, sample volumes were scaled to achieve ~10 mg of dry mass after drying, and drying times modulated to achieve ~11% water content after drying, verified by Karl–Fischer coulometry. After drying, samples were loaded into Tzero pans, the samples' mass determined, and then hermetically sealed. Runs consisted of a 30-min isothermal hold at −40 °C, before a 2 °C/min ramp to 100 °C. Glass transition was selected, and the Tg onset, midpoint, and offset were determined via TA instruments Trios software, utilizing built-in onset and endset analysis. m-index was then calculated utilizing equations 10 and 14 from ref. 73. Where m is the alternative fragility parameter, T_g is the glass transition temperature onset, T_g^{off} is the glass transition offset temperature, ΔE_{T_g} is the activation enthalpy of structural relaxation at T_g, R is the gas constant, and ΔE_η is the activation

enthalpy for viscosity. Constant is an empirical constant of 5 ± 0.5, and m can be solved assuming ΔE_{T_g} and ΔE_η are equivalent[73].

$$m = \frac{\Delta E_{T_g}}{(\ln 10) R T_g} \quad (1)$$

$$constant = \left(\frac{\Delta E_\eta}{R}\right)\left(\frac{1}{T_g} - \frac{1}{T_g^{off}}\right) \quad (2)$$

Data availability

The authors declare that all data supporting the findings of this study are available within the paper and its supplementary information file (Supplementary Data 1).

Received: 17 December 2024; Accepted: 11 June 2025;
Published online: 01 July 2025

References

1. Gote, V. et al. A comprehensive review of mRNA vaccines. *Int. J. Mol. Sci.* **24**, 2700 (2023).
2. Cheng, F. et al. Research advances on the stability of mRNA vaccines. *Viruses* **15**, 668 (2023).
3. Chheda, U. et al. Factors affecting stability of RNA – temperature, length, concentration, pH, and buffering species. *J. Pharm. Sci.* **113**, 377–385 (2024).
4. Kong, Q. & Lin, C.-L. G. Oxidative damage to RNA: mechanisms, consequences, and diseases. *Cell. Mol. Life Sci.* **67**, 1817–1829 (2010).
5. Li, Y. & Breaker, R. R. Kinetics of RNA degradation by specific base catalysis of transesterification involving the 2'-hydroxyl group. *J. Am. Chem. Soc.* **121**, 5364–5372 (1999).
6. Soukup, G. A. & Breaker, R. R. Relationship between internucleotide linkage geometry and the stability of RNA. *RNA* **5**, 1308–1325 (1999).
7. Fabre, A.-L., Colotte, M., Luis, A., Tuffet, S. & Bonnet, J. An efficient method for long-term room temperature storage of RNA. *Eur. J. Hum. Genet.* **22**, 379–385 (2014).
8. Wan, E. et al. Green technologies for room temperature nucleic acid storage. *Curr. Issues Mol. Biol.* **12**, 135–142 (2010).
9. Seelenfreund, E. et al. Long term storage of dry versus frozen RNA for next generation molecular studies. *PLoS ONE* **9**, e111827 (2014).
10. Cayuela, J.-M. et al. A novel method for room temperature distribution and conservation of RNA and DNA reference materials for guaranteeing performance of molecular diagnostics in onco-hematology: a GBMHM study. *Clin. Biochem.* **48**, 982–987 (2015).
11. Merivaara, A. et al. Preservation of biomaterials and cells by freeze-drying: change of paradigm. *J. Control. Release* **336**, 480–498 (2021).
12. Packebush, M. H. et al. Natural and engineered mediators of desiccation tolerance stabilize human blood clotting factor VIII in a dry state. *Sci. Rep.* **13**, 4542 (2023).
13. Piszkiewicz, S. et al. Protecting activity of desiccated enzymes. *Protein Sci.* **28**, 941–951 (2019).
14. Ohtake, S. & Wang, Y. J. Trehalose: current use and future applications. *J. Pharm. Sci.* **100**, 2020–2053 (2011).
15. Chen, Y., Mutukuri, T. T., Wilson, N. E. & Zhou, Q. T. Pharmaceutical protein solids: drying technology, solid-state characterization and stability. *Adv. Drug Deliv. Rev.* **172**, 211–233 (2021).
16. Liao, Y.-H., Brown, M. B., Quader, A. & Martin, G. P. Protective mechanism of stabilizing excipients against dehydration in the freeze-drying of proteins. *Pharm. Res.* **19**, 1854–1861 (2002).
17. Ivanova, N. V. & Kuzmina, M. L. Protocols for dry DNA storage and shipment at room temperature. *Mol. Ecol. Resour.* **13**, 890–898 (2013).
18. Marrone, A. & Ballantyne, J. Hydrolysis of DNA and its molecular components in the dry state. *Forensic Sci. Int. Genet.* **4**, 168–177 (2010).
19. Rajjou, L. et al. The effect of alpha-amanitin on the Arabidopsis seed proteome highlights the distinct roles of stored and neosynthesized mRNAs during germination. *Plant Physiol.* **134**, 1598–1613 (2004).
20. Sano, N. et al. Accumulation of long-lived mRNAs associated with germination in embryos during seed development of rice. *J. Exp. Bot.* **66**, 4035–4046 (2015).
21. Wolniak, S. M., van der Weele, C. M., Deeb, F., Boothby, T. & Klink, V. P. Extremes in rapid cellular morphogenesis: post-transcriptional regulation of spermatogenesis in *Marsilea vestita*. *Protoplasma* **248**, 457–473 (2011).
22. Waters, L. C. & Dure, L. S. 3rd. Ribonucleic acid synthesis in germinating cotton seeds. *J. Mol. Biol.* **19**, 1–27 (1966).
23. Saighani, K. et al. Correlation between seed longevity and RNA integrity in the embryos of rice seeds. *Plant Biotechnol.* **38**, 277–283 (2021).
24. Fleming, M. B., Richards, C. M. & Walters, C. Decline in RNA integrity of dry-stored soybean seeds correlates with loss of germination potential. *J. Exp. Bot.* **68**, 2219–2230 (2017).
25. Clegg, J. S. & Golub, A. L. Protein synthesis in *Artemia salina* embryos. II. Resumption of RNA and protein synthesis upon cessation of dormancy in the encysted gastrula. *Dev. Biol.* **19**, 178–200 (1969).
26. Crowe, J. H., Hoekstra, F. A. & Crowe, L. M. Anhydrobiosis. *Annu. Rev. Physiol.* **54**, 579–599 (1992).
27. Koster, K. L. & Leopold, A. C. Sugars and desiccation tolerance in seeds. *Plant Physiol.* **88**, 829–832 (1988).
28. Hibshman, J. D., Clegg, J. S. & Goldstein, B. Mechanisms of desiccation tolerance: themes and variations in brine shrimp, roundworms, and tardigrades. *Front. Physiol.* **11**, 592016 (2020).
29. Potts, M. Desiccation tolerance of prokaryotes. *Microbiol. Rev.* **58**, 755–805 (1994).
30. Womersley, C. Biochemical and physiological aspects of anhydrobiosis. *Comp. Biochem. Physiol. B Comp. Biochem.* **70**, 669–678 (1981).
31. MacRae, T. H. Molecular chaperones, stress resistance and development in *Artemia franciscana*. *Semin. Cell Dev. Biol.* **14**, 251–258 (2003).
32. Tapia, H. & Koshland, D. E. Trehalose is a versatile and long-lived chaperone for desiccation tolerance. *Curr. Biol.* **24**, 2758–2766 (2014).
33. Erkut, C. et al. Trehalose renders the dauer larva of *Caenorhabditis elegans* resistant to extreme desiccation. *Curr. Biol.* **21**, 1331–1336 (2011).
34. Crowe, J. H. in *Molecular Aspects of the Stress Response: Chaperones, Membranes and Networks* (eds. Csermely, P. & Vígh, L.) (Springer, 2007).
35. Tapia, H., Young, L., Fox, D., Bertozzi, C. R. & Koshland, D. Increasing intracellular trehalose is sufficient to confer desiccation tolerance to Saccharomyces cerevisiae. *Proc. Natl Acad. Sci. USA* **112**, 6122–6127 (2015).
36. Drennan, P. M., Smith, M. T., Goldsworthy, D. & van Staden, J. The occurrence of trehalose in the leaves of the desiccation-tolerant angiosperm *Myrothamnus flabellifolius* welw. *J. Plant Physiol.* **142**, 493–496 (1993).
37. Billi, D. et al. Engineering desiccation tolerance in *Escherichia coli*. *Appl. Environ. Microbiol.* **66**, 1680–1684 (2000).
38. Halperin, S. J. & Koster, K. L. Sugar effects on membrane damage during desiccation of pea embryo protoplasts. *J. Exp. Bot.* **57**, 2303–2311 (2006).
39. Crowe, J. H., Crowe, L. M., Carpenter, J. F. & Aurell Wistrom, C. Stabilization of dry phospholipid bilayers and proteins by sugars. *Biochem. J.* **242**, 1–10 (1987).
40. Leslie, S. B., Teter, S. A., Crowe, L. M. & Crowe, J. H. Trehalose lowers membrane phase transitions in dry yeast cells. *Biochim. Biophys. Acta Biomembr.* **1192**, 7–13 (1994).

41. Gervasi, V. et al. Parenteral protein formulations: an overview of approved products within the European Union. *Eur. J. Pharm. Biopharm.* **131**, 8–24 (2018).
42. Julca, I., Alaminos, M., González-López, J. & Manzanera, M. Xeroprotectants for the stabilization of biomaterials. *Biotechnol. Adv.* **30**, 1641–1654 (2012).
43. Jones, K. L., Drane, D. & Gowans, E. J. Long-term storage of DNA-free RNA for use in vaccine studies. *Biotechniques* **43**, 675–681 (2007).
44. Neo, S. H., Chung, K. Y., Quek, J. M. & Too, H.-P. Trehalose significantly enhances the recovery of serum and serum exosomal miRNA from a paper-based matrix. *Sci. Rep.* **7**, 16686 (2017).
45. Schroeder, A. et al. The RIN: an RNA integrity number for assigning integrity values to RNA measurements. *BMC Mol. Biol.* **7**, 3 (2006).
46. Carpenter, J. F. & Crowe, J. H. An infrared spectroscopic study of the interactions of carbohydrates with dried proteins. *Biochemistry* **28**, 3916–3922 (1989).
47. Ramirez, J. F., Kumara, U. G. V. S. S., Arulsamy, N. & Boothby, T. C. Water content, transition temperature and fragility influence protection and anhydrobiotic capacity. *BBA Adv.* **5**, 100115 (2024).
48. Ballesteros, D. & Walters, C. Solid-state biology and seed longevity: a mechanical analysis of glasses in pea and soybean embryonic axes. *Front. Plant Sci.* **10**, 920 (2019).
49. Brown, G. M. & Levy, H. A. Further refinement of the structure of sucrose based on neutron-diffraction data. *Acta Crystallogr. B* **29**, 790–797 (1973).
50. Lee, T. & Chang, G. D. Sucrose conformational polymorphism: a jigsaw puzzle with multiple routes to a unique solution. *Cryst. Growth Des.* **9**, 3551–3561 (2009).
51. Malferrari, M. et al. Structural and dynamical characteristics of trehalose and sucrose matrices at different hydration levels as probed by FTIR and high-field EPR. *Phys. Chem. Chem. Phys.* **16**, 9831–9848 (2014).
52. Nagase, H., Endo, T., Ueda, H. & Nakagaki, M. An anhydrous polymorphic form of trehalose. *Carbohydr. Res.* **337**, 167–173 (2002).
53. Raimi-Abraham, B. T., Moffat, J. G., Belton, P. S., Barker, S. A. & Craig, D. Q. M. Generation and characterization of standardized forms of trehalose dihydrate and their associated solid-state behavior. *Cryst. Growth Des.* **14**, 4955–4967 (2014).
54. Nunes, C., Mahendrasingam, A. & Suryanarayanan, R. Quantification of crystallinity in substantially amorphous materials by synchrotron X-ray powder diffractometry. *Pharm. Res.* **22**, 1942–1953 (2005).
55. Booth, A. & Hay, J. N. The use of differential scanning calorimetry to study polymer crystallization kinetics. *Polymer* **10**, 95–104 (1969).
56. Yin, L., Wang, J., Lin, T. & You, J. Inclusion/exclusion behaviors of small molecules during crystallization of polymers in miscible PLLA/TAIC blend. *Polymers* **14**, 2737 (2022).
57. Bonnet, J. et al. Chain and conformation stability of solid-state DNA: implications for room temperature storage. *Nucleic Acids Res.* **38**, 1531–1546 (2010).
58. Yoshioka, M., Hancock, B. C. & Zografi, G. Crystallization of indomethacin from the amorphous state below and above its glass transition temperature. *J. Pharm. Sci.* **83**, 1700–1705 (1994).
59. Perrin, D. D. & Armarego, W. *Purification of Laboratory Chemicals* (Butterworth-Heinemann, 1966).
60. Powers, H. E. C. Sucrose crystal inclusions. *Nature* **182**, 715–717 (1958).
61. Carstensen, J. T. & Van Scoik, K. Amorphous-to-crystalline transformation of sucrose. *Pharm. Res.* **7**, 1278–1281 (1990).
62. Kilburn, D. et al. Organization and mobility of water in amorphous and crystalline trehalose. *Nat. Mater.* **5**, 632–635 (2006).
63. Ahlqvist, M. U. A. & Taylor, L. S. Water diffusion in hydrated crystalline and amorphous sugars monitored using H/D exchange. *J. Pharm. Sci.* **91**, 690–698 (2002).
64. Shirakashi, R. & Takano, K. Recrystallization and water absorption properties of vitrified trehalose near room temperature. *Pharm. Res.* **35**, 139 (2018).
65. Auffinger, P. & Westhof, E. Hydration of RNA base pairs. *J. Biomol. Struct. Dyn.* **16**, 693–707 (1998).
66. Kirillova, S. & Carugo, O. Hydration sites of unpaired RNA bases: a statistical analysis of the PDB structures. *BMC Struct. Biol.* **11**, 41 (2011).
67. Crowe, J. H., Clegg, J. S. & Crowe, L. M. Anhydrobiosis: the water replacement hypothesis. In *The Properties of Water in Foods ISOPOW 6* (ed. Reid, D. S.) (Springer, 1998).
68. Jain, N. K. & Roy, I. Effect of trehalose on protein structure. *Protein Sci.* **18**, 24–36 (2009).
69. Bezrukavnikov, S. et al. Trehalose facilitates DNA melting: a single-molecule optical tweezers study. *Soft Matter* **10**, 7269–7277 (2014).
70. Lambert, D. & Draper, D. E. Effects of osmolytes on RNA secondary and tertiary structure stabilities and RNA-Mg2+ interactions. *J. Mol. Biol.* **370**, 993–1005 (2007).
71. Hoekstra, F. A. & van Roekel, T. Desiccation tolerance of *Papaver dubium* L. pollen during its development in the anther: possible role of phospholipid composition and sucrose content. *Plant Physiol.* **88**, 626–632 (1988).
72. Sano, F., Asakawa, N., Inoue, Y. & Sakurai, M. A dual role for intracellular trehalose in the resistance of yeast cells to water stress. *Cryobiology* **39**, 80–87 (1999).
73. Crowley, K. J. & Zografi, G. The use of thermal methods for predicting glass-former fragility. *Thermochim. Acta* **380**, 79–93 (2001).

Acknowledgements

pET28a:GFP was a gift from Matthew Bennett (Addgene plasmid # 60733;http://n2t.net/addgene:60733; RRID:Addgene_60733). This research was supported in part by the USDA National Institute of Food and Agriculture, Hatch project #1012152. In addition, this work was made possible in part through support from an Institutional Development Award (IDeA) from the National Institute of General Medical Sciences of the National Institutes of Health (Grant # 2P20GM103432) and the NSF (CHE 0619920). This work was also supported by an NSF DBI grant #2213983 to Thomas Boothby via the Water and Life Interface Institute (WALII). We thank WALII members for their input and helpful discussions.

Author contributions

Conceptualization, methodology, writing—original draft and writing—reviewing and editing: T.C.B. and T.J.G. Data curation, formal analysis, investigation and visualization: T.J.G. Funding acquisition, project administration and supervision: TCB.

Competing interests

TCB and TJG are listed as inventors on an institutional provisional patent UWYO/0137USL, which covers aspects of sugar-based stabilization of RNA in the dry state.

Additional information

Supplementary information The online version contains supplementary material available at https://doi.org/10.1038/s43246-025-00850-y.

Correspondence and requests for materials should be addressed to Thomas C. Boothby.

Peer review information *Communications Materials* thanks Jack Douglas, Marcus T. Cicerone, Urmi Chheda and the other, anonymous, reviewer(s) for their contribution to the peer review of this work. Primary Handling Editors: Jet-Sing Lee. [A peer review file is available.]